Hindawi Publishing Corporation
Journal of Nanomaterials
Volume 2015, Article ID 230987, 7 pages
http://dx.doi.org/10.1155/2015/230987

Research Article

Vertical Graphene Nanosheets Coated with Gold Nanoparticle Arrays: Effect of Interparticle Spacing on Optical Response

Angus Mcleod,[1] Shailesh Kumar,[2] Kristy C. Vernon,[1] and Kostya (Ken) Ostrikov[1,2,3]

[1]*School of Chemistry, Physics, and Mechanical Engineering and Institute for Future Environments, Queensland University of Technology, GPO Box 2434, Brisbane, QLD 4001, Australia*
[2]*Manufacturing Flagship, Commonwealth Scientific and Industrial Research Organization, P.O. Box 218, Lindfield, NSW 2070, Australia*
[3]*Plasma Nanoscience, Complex Systems, University of Sydney, Sydney, NSW 2006, Australia*

Correspondence should be addressed to Kristy C. Vernon; k.vernon@qut.edu.au

Received 19 December 2014; Accepted 6 March 2015

Academic Editor: Venkatram Nalla

Vertical graphene nanosheets have advantages over their horizontal counterparts, primarily due to the larger surface area available in the vertical systems. Vertical sheets can accommodate more functional particles, and, due to the conduction and optical properties of thin graphene, these structures can find niche applications in the development of sensing and energy storage devices. This work is a combined experimental and theoretical study that reports on the synthesis and optical responses of vertical sheets decorated with gold nanoparticles. The findings help in interpreting optical responses of these hybrid graphene structures and are relevant to the development of future sensing platforms.

1. Introduction

Graphenes consist of a small number of atomic carbon layers arranged in a hexagonal lattice. Graphene has unique optical and electrical properties [1–5], making graphene-based systems of vital importance for the creation of the next generation of optical sensors, photovoltaics, and energy storage devices [2–4, 6–13]. Graphene architectures can take many forms, from carbon flakes [14, 15], carbon nanotubes [4, 14], horizontal sheets [3, 4], and vertical graphene nanosheets (VGNs) [2, 4, 6, 7, 12–14, 16–20].

VGNs typically consist of a few vertically oriented atomic carbon layers produced via plasma enhanced chemical vapour deposition [2, 4, 12–14, 16–21]. VGNs represent a unique vertically oriented graphene-based architecture due to their large surface area compared to their horizontal counterparts [4, 6, 7]. Functional particles can be added to both sides of the VGN, and the interaction between these particles can be controlled by altering the number of graphene sheets making up the VGN [4, 6, 7].

This combination of large surface area and control of interparticle coupling makes VGNs decorated with functional materials promising candidates for the development of new hybrid materials. Such materials can display exotic physical properties that are not seen in the individual elements making up the hybrid material. For example, when metal nanoparticles are combined with carbon nanotubes, the new hybrid structures display electron transport properties not seen in either of the constituents [4, 22]. Due to the exotic properties of hybrid materials, the new hybrid nanomaterials may significantly advance optical sensing and energy storage applications [2, 4, 7, 13, 22].

Graphenes are relatively low-loss and transparent optical materials which can provide strong electromagnetic (EM) confinement, making the interaction of graphene with metal nanoparticles of interest for the development of novel plasmonic-based devices [4, 6, 23]. In particular, decorating graphene with metallic nanostructures has led to the development of new surface enhanced Raman spectroscopy (SERS) systems [7, 8, 24–27]. The metal nanoparticles can focus

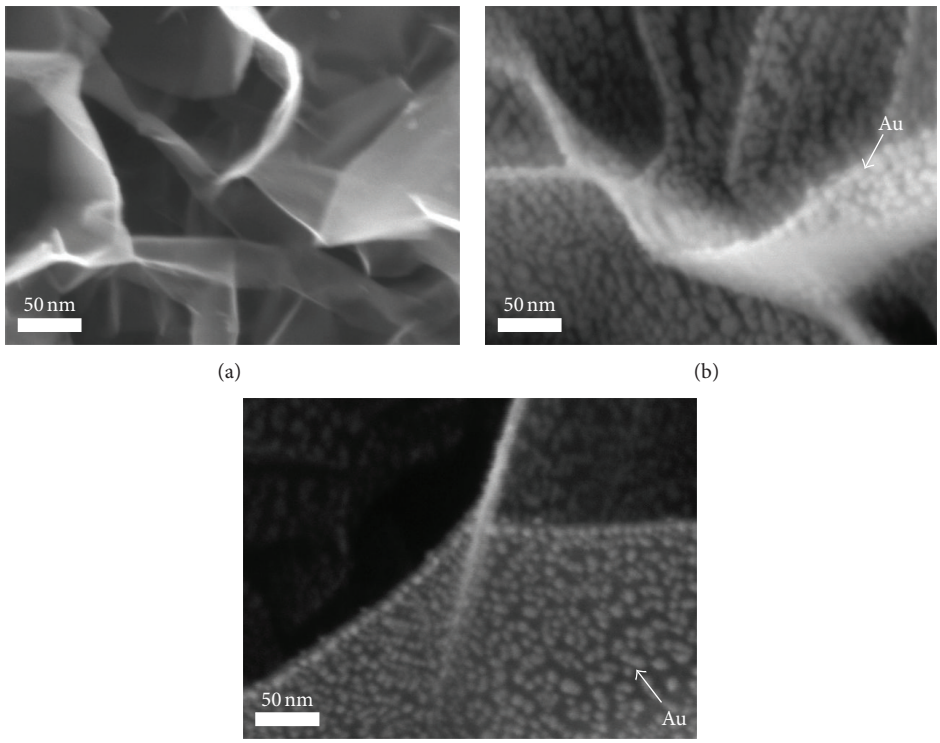

Figure 1: (a) SEM of uncoated VGN, (b) Au nanoparticle coated VGN edge, and (c) side-view of the Au nanoparticle coated vertical walls of the VGN.

the light down to nanoscale areas, increasing the SERS signal intensity.

Gold nanoparticle-decorated VGNs are a hybrid plasmonic system which could find applications in optical and SERS sensing. This paper studies the optical properties of these gold nanoparticle-decorated VGN systems synthesised by plasma enhanced chemical vapour deposition (PECVD), using a combination of optical microscopy, Raman spectroscopy, and theoretical finite element analysis models.

2. Materials and Methods

The VGNs were fabricated on a Si(100) substrate using a low-temperature, low-pressure PECVD process. The substrate was first pretreated by exposure to N_2 plasma for 5 min (N_2 inlet 50 sccm, microwave power 500 W, and chamber pressure 7 Torr) and the substrate reached a temperature of approximately 400°C. After the treatment, 10 minutes of deposition was performed using the following process parameters: CH_4/N_2 gas inlet ratio of 1 : 1, input power of 750 W, and chamber pressure of 10 Torr. The final temperature of the substrate at the end of deposition was approximately ~800°C. Further information on the relevant fabrication processes can be found elsewhere [7].

Gold nanoparticles were then thermally evaporated onto the VGN at room temperature. The process parameters used were the following: filament temperature ~1620°C, distance between the sample and filament ~25 cm, 0.5 mm diameter of mesh between the sample and filament, mesh thickness ~1 mm, distance between mesh and sample ~1 mm, and chamber pressure 2.0×10^{-6} Torr. For further details of the process, see [7].

SEM images of the resultant gold-decorated VGNs are shown in Figure 1. These SEM images were taken using a Zeiss Ultra Plus Scanning Electron Microscope operated at 4 kV accelerating voltage. It is clear from Figure 1(b) that the gold nanoparticles coat both sides of the sheet.

The density of the gold nanoparticles on the VGNs varied from distance of the specific sample areas from the evaporation orifice. Four samples were considered with varying distance to the evaporation orifice. This was done by mounting the VGN samples radially from the center of the mesh hole [7]. The fourth sample was directly beneath the mesh hole. SEM images of the four samples are shown in Figure 2.

The SEM images of the four samples were analysed and the density of particles and particle size are given in Table 1.

3. Results and Discussion

3.1. Optical Properties of Gold-Coated Vertical Graphenes. The optical properties of the gold-coated VGNs changed significantly depending on the density of the gold nanoparticles. Various densities of gold nanoparticles were deposited on the VGN, and CCD camera images of the samples were taken using a Renishaw *inVia* Raman Microscope, Figure 3. As can be seen from Figure 3, increasing the density of the gold nanoparticles ((a)–(d)) results in a change to the wavelength

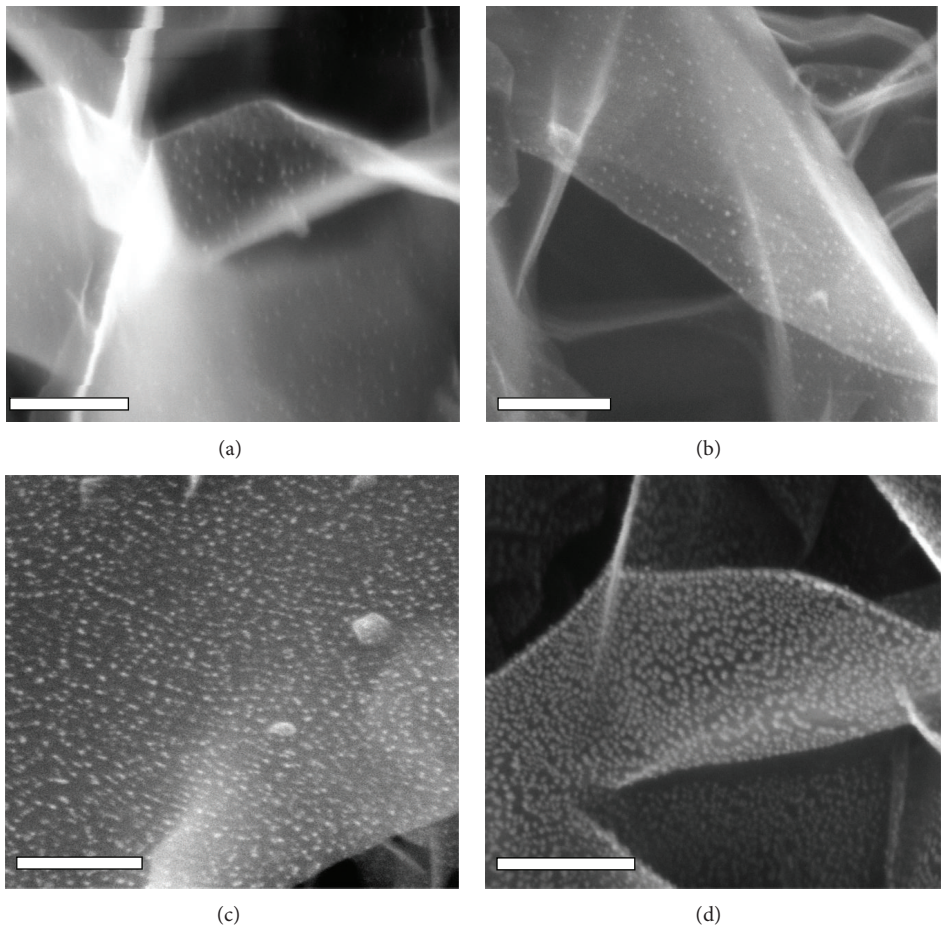

Figure 2: (a–c) SEM images show denser patterns of Au NPs thermally deposited on VGN as moving radially towards the center of the mesh hole. (d) A dense pattern of larger Au NPs on VGN close to the center of the mesh.

Table 1: Average particle diameter and number of particles per nm^2 for four samples.

Sample	Average particle diameter (nm)	Nanoparticles/area ($\times 10^{-3}/nm^2$)
1	11 ± 1	6 ± 1
2	10 ± 1	9 ± 1
3	11 ± 2	13 ± 1
4	14 ± 3	22 ± 3

of light scattered from the VGN surface. This indicates that the density of the nanoparticles, as well as the interparticle spacing, significantly affects the optical properties of the Au-VGN hybrid structure.

Using the Renishaw *inVia* Raman Microscope (with a 1 mW 633 nm laser excitation source, room temperature, and spot size 1 μm diameter) micro-Raman spectra were acquired from the observably highest concentration of Au nanoparticles on various samples. A 100x objective lens was used in the spectra collection. A noncoated VGN was also characterized for comparison. The spectra are given in Figure 4. The blue and green curves correspond to samples 2 and 3 and the brown curve corresponds to sample 4. Two intense Raman peaks, a sharp graphitic G-peak (1584 cm^{-1}) and a second order 2D-peak (2662 cm^{-1}), and two low-intensity peaks, disorder-related D-peak (1338 cm^{-1}) and (D + G)-peak (2934 cm^{-1}), were observed in the spectra.

Clearly, decorating the VGNs with gold nanoparticles results in a stronger SERS signal as compared to pristine VGNs. Main peak positions also experienced a slight shift between the areas of different Au nanoparticle density, that is, where interparticle distances were different.

From the optical images and Raman spectra, it is clear that the interparticle spacing between the gold nanoparticles affects the optical properties of the hybrid gold-decorated VGN structure. Furthermore, these hybrid graphene structures have promising applications in optical sensing, as can be seen in Figure 3.

The Raman spectra in Figure 4 clearly show stronger intensity of activated radial breathing-like mode (RB-LM) at 296 cm^{-1} of VGN with denser patterns of Au NPs. This suggests that optical property of graphene is enhanced. However, the scattering from the gold nanoparticle assemblies also contributes to the background intensity.

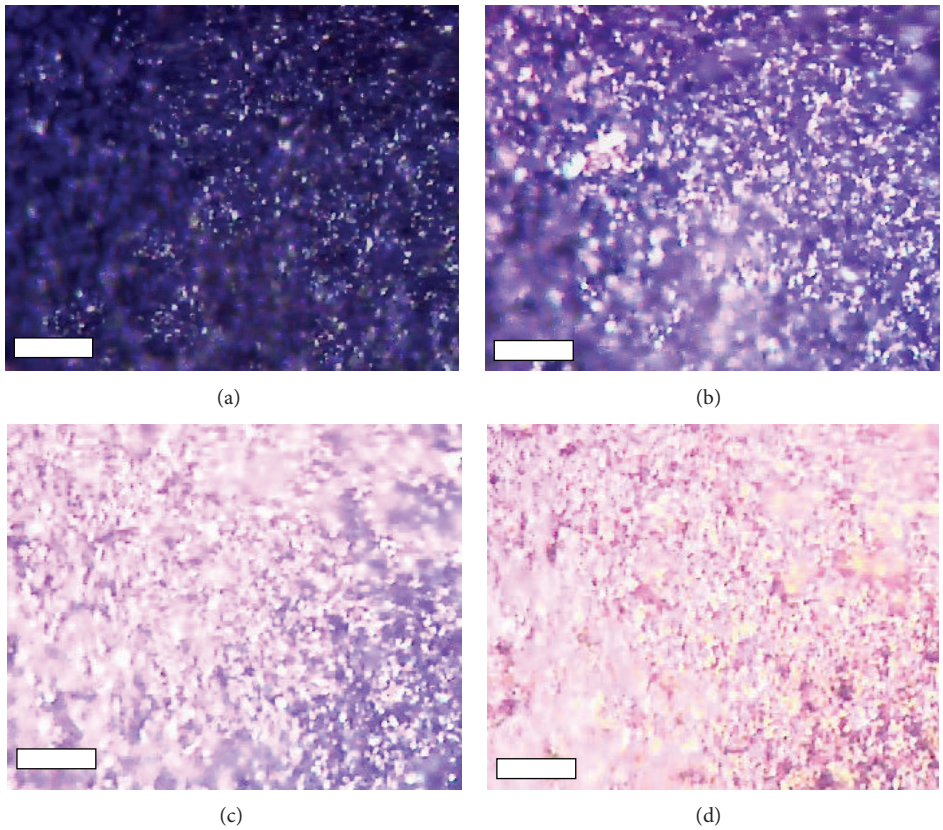

Figure 3: Optical images of increasing density (a–d) of Au nanoparticles on VGN sheets. The scale bar in all images is 5 μm.

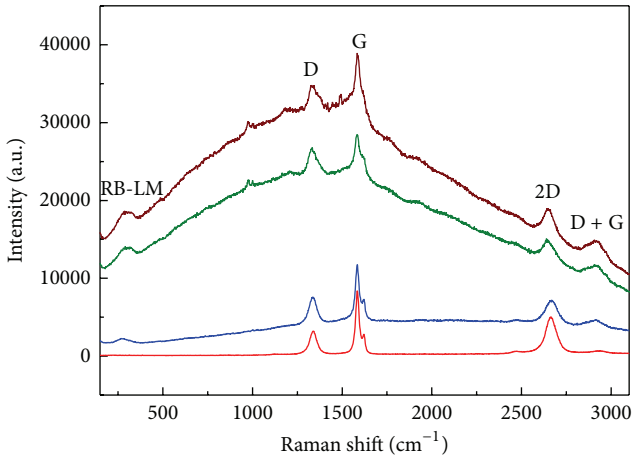

Figure 4: Representative Raman spectra (1 s acquisition time) for gold nanoparticle-decorated VGNs (blue, green, and brown) and for undecorated VGNs (red).

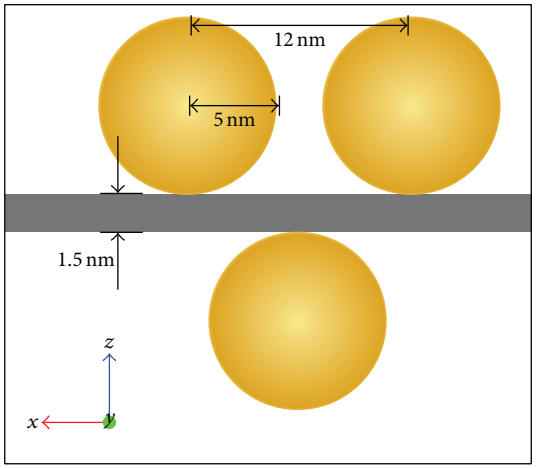

Figure 5: Schematic of the gold trimer system on the vertical graphene sheet of approximately 5 atomic carbon layers. The separation distance between the top particles is 12 nm in this diagram.

To understand why the Au nanoparticle presence (and density) on both sides of the vertical graphene sheets affects the optical properties of the VGN structures, numerical modeling of the optical responses of these hybrid structures has been performed using COMSOL Multiphysics.

The gold nanoparticles are modelled as 10 nm diameter spheres atop 1.5 nm (approximately five atomic carbon layers) graphene sheet. The optical properties of gold and few-layer graphenes were taken from Palik [28] and Weber et al. [29], respectively. A trimer configuration is considered (Figure 5) as a close approximation to a small section of the VGN decorated with Au nanoparticles. The trimer consists of two particles on one side of the sheet and the third particle on

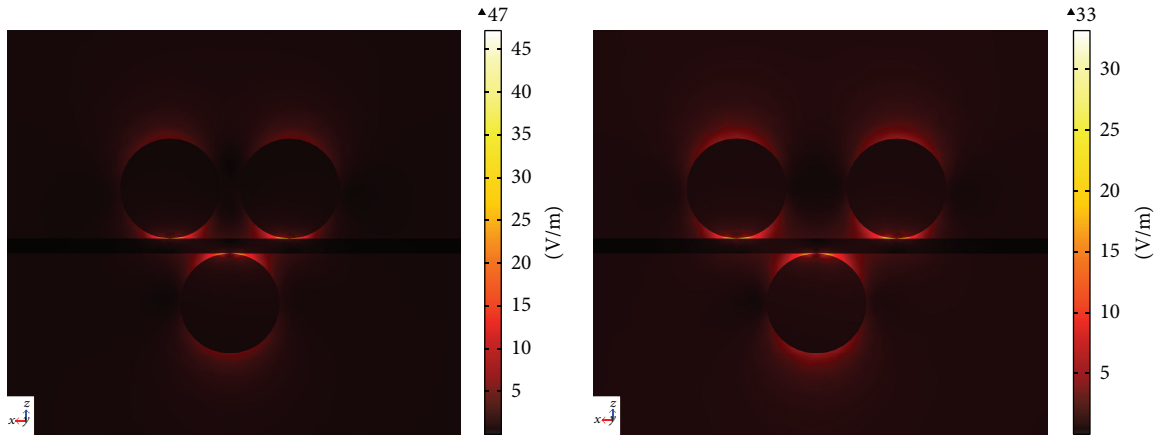

(a) (b)

Figure 6: $|E|$ for interparticle separation of (a) 12 nm and (b) 16 nm.

Table 2: Maximum SERS signal for various nanoparticle separation distances.

Separation (nm)	SERS signal ($\times 10^6$)
12	5.89
14	2.28
16	1.27

the opposing side of the sheet. The separation between the two particles on the same side of the sheet is varied, to investigate how the particle density affects the SERS signal (Figure 5). The separation between the particles is varied from 12 nm to 16 nm center to center, to approximate changing densities as seen in the experiment.

Two types of incident beam are considered: (1) beam polarised in x and propagating along z direction and (2) beam polarised in z and propagating along x direction. Due to the relative scales of the graphene compared to the nanoparticles, the graphene is treated as an infinite plane and perfectly matched layers are used as the boundaries. The far-field is calculated using the Stratton-Chu formulation. The models are based on classical physics and do not take into account quantum mechanical effects that may affect signal intensity, as well as peak number/quantization and locations [30, 31]. A more robust approach addressing the quantum effects and accounting for losses due to optical phonon coupling and defects [32] will be the subject of future work.

3.2. Results of Theory Modeling. In the trimer system, the resonance peak is obtained at 531 nm with the maximal SERS signal at resonance recorded for the 12 nm separation. The SERS signal peak is ~5.9×10^6 which is stronger than the case of a single isolated gold nanoparticle on a graphene sheet [6] and indicates why it is important to use VGNs where both sides of the sheet can be coated. The SERS signal peaks for various separation distances are given in Table 2.

As expected, the SERS signal strength decreases with increasing the interparticle distance. This is clear from

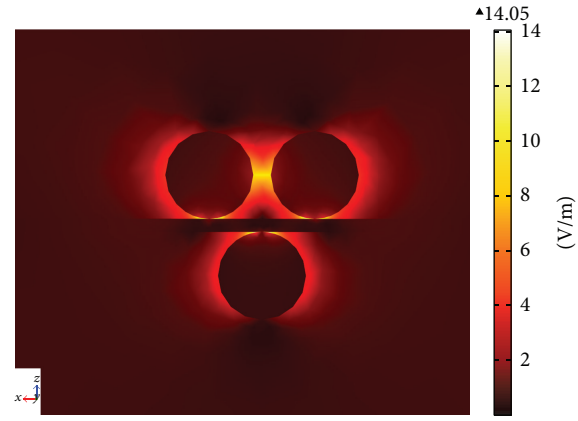

Figure 7: $|E|$ for interparticle separation of 12 nm, x polarization.

the electric field distribution ($|E|$) of the trimer at resonance (Figure 6). The main field strength lies at the contact point between the nanoparticle and the graphene sheet, with interparticle coupling playing a relatively minor role. Increasing the separation distance leads to smaller field intensities as the particles experience weaker coupling to the third particle through the graphene sheet.

However, this was for the beam incident in the x direction. When the trimers were analyzed for an incident beam in z direction, the SERS signal was much weaker. Indeed, in the case of a 12 nm separation, the SERS signal strength was only ~4.6×10^4, about 100 times weaker than the SERS signal in the case of the beam incident in the x direction. This is also evident from the electric field plot, Figure 7. The field is mostly concentrated between the particles on the same side of the sheet, with weaker signal coupling through the VGN. This makes the overall field strength and the SERS signal weaker than in the other polarization case.

Possible future avenues of theoretical study would be to test infinite arrays of these gold nanoparticles to determine the influence an ordered system has on the resultant SERS

signal. Methods of increasing the SERS signal, such as by altering the particle geometry, decreasing the number of sheets in the VGN, or introducing further close packed particles might also be considered to better understand the effect of the contact region on the resultant optical response.

4. Conclusions

Decoration of VGNs with gold nanoparticles results in a unique 3D hybrid graphene-gold architecture which provides a strong SERS signal as opposed to uncoated VGNs. The density of the gold nanoparticles on the VGNs directly affects the optical properties and the resultant maximum SERS signal that can be obtained from these hybrid structures. Coupling between the gold nanoparticles and the graphene sheet should be optimized for achieving the maximum SERS signal enhancement. A viable option is to control positions, sizes, and densities of gold nanoparticles on both sides of the vertical graphene sheets. These results are relevant to the development of the next-generation optical sensing platforms based on localized plasmonic and SERS responses to various optical excitations and analyzed species.

Conflict of Interests

The authors declare that there is no conflict of interests regarding the publication of this paper.

Acknowledgments

Angus Mcleod acknowledges support from the QUT HPC team. Angus Mcleod and Kristy C. Vernon acknowledge the Australian Research Council (ARC) Grant DP110101454. Angus Mcleod and Shailesh Kumar acknowledge support from CSIRO's Sensor and Sensor Networks TCP. Shailesh Kumar and Kostya (Ken) Ostrikov acknowledge support from the CSIRO Office of Chief Executive Science Leadership Program and the ARC.

References

[1] D. S. L. Abergel, V. Apalkov, J. Berashevich, K. Ziegler, and T. Chakraborty, "Properties of graphene: a theoretical perspective," *Advances in Physics*, vol. 59, no. 4, pp. 261–482, 2010.

[2] D. H. Seo, S. Kumar, and K. Ostrikov, "Control of morphology and electrical properties of self-organized graphenes in a plasma," *Carbon*, vol. 49, no. 13, pp. 4331–4339, 2011.

[3] S. Guo and S. Dong, "Graphene nanosheet: synthesis, molecular engineering, thin film, hybrids, and energy and analytical applications," *Chemical Society Reviews*, vol. 40, no. 5, pp. 2644–2672, 2011.

[4] K. Ostrikov, E. C. Neyts, and M. Meyyappan, "Plasma nanoscience: from nano-solids in plasmas to nano-plasmas in solids," *Advances in Physics*, vol. 62, no. 2, pp. 113–224, 2013.

[5] Z. Yang, R. Gao, N. Hu et al., "The prospective two-dimensional graphene nanosheets: preparation, functionalization, and applications," *Nano-Micro Letters*, vol. 4, no. 1, pp. 1–9, 2012.

[6] A. McLeod, K. C. Vernon, A. E. Rider, and K. Ostrikov, "Optical coupling of gold nanoparticles on vertical graphenes to maximize SERS response," *Optics Letters*, vol. 39, no. 8, pp. 2334–2337, 2014.

[7] A. E. Rider, S. Kumar, S. A. Furman, and K. K. Ostrikov, "Self-organized Au nanoarrays on vertical graphenes: an advanced three-dimensional sensing platform," *Chemical Communications*, vol. 48, no. 21, pp. 2659–2661, 2012.

[8] C.-E. Cheng, C.-Y. Lin, H.-Y. Chang et al., "Surface-enhanced Raman scattering of graphene with photo-assisted- synthesized gold nanoparticles," *Optics Express*, vol. 21, no. 5, pp. 6547–6554, 2013.

[9] P. K. Maharana, T. Srivastava, and R. Jha, "Ultrasensitive plasmonic imaging sensor based on graphene and silicon," *IEEE Photonics Technology Letters*, vol. 25, no. 2, pp. 122–125, 2013.

[10] M. M. Giangregorio, M. Losurdo, G. V. Bianco, E. Dilonardo, P. Capezzuto, and G. Bruno, "Synthesis and characterization of plasmon resonant gold nanoparticles and graphene for photovoltaics," *Materials Science and Engineering B: Solid-State Materials for Advanced Technology*, vol. 178, no. 9, pp. 559–567, 2013.

[11] D. A. C. Brownson and C. E. Banks, "Fabricating graphene supercapacitors: highlighting the impact of surfactants and moieties," *Chemical Communications*, vol. 48, no. 10, pp. 1425–1427, 2012.

[12] Z. Bo, W. Zhu, W. Ma et al., "Vertically oriented graphene bridging active-layer/current-collector interface for ultrahigh rate supercapacitors," *Advanced Materials*, vol. 25, no. 40, pp. 5799–5806, 2013.

[13] M. Cai, R. A. Outlaw, S. M. Butler, and J. R. Miller, "A high density of vertically-oriented graphenes for use in electric double layer capacitors," *Carbon*, vol. 50, no. 15, pp. 5481–5488, 2012.

[14] O. Volotskova, I. Levchenko, A. Shashurin, Y. Raitses, K. Ostrikov, and M. Keidar, "Single-step synthesis and magnetic separation of graphene and carbon nanotubes in arc discharge plasmas," *Nanoscale*, vol. 2, no. 10, pp. 2281–2285, 2010.

[15] I. Levchenko, O. Volotskova, A. Shashurin, Y. Raitses, K. Ostrikov, and M. Keidar, "The large-scale production of graphene flakes using magnetically-enhanced arc discharge between carbon electrodes," *Carbon*, vol. 48, no. 15, pp. 4570–4574, 2010.

[16] J. Zhao, M. Shaygan, J. Eckert, M. Meyyappan, and M. H. Rümmeli, "A growth mechanism for free-standing vertical graphene," *Nano Letters*, vol. 14, no. 6, pp. 3064–3071, 2014.

[17] Z. Bo, Y. Yang, J. Chen, K. Yu, J. Yan, and K. Cen, "Plasma-enhanced chemical vapor deposition synthesis of vertically oriented graphene nanosheets," *Nanoscale*, vol. 5, no. 12, pp. 5180–5204, 2013.

[18] J. Wang, M. Zhu, R. A. Outlaw, X. Zhao, D. M. Manos, and B. C. Holloway, "Synthesis of carbon nanosheets by inductively coupled radio-frequency plasma enhanced chemical vapor deposition," *Carbon*, vol. 42, no. 14, pp. 2867–2872, 2004.

[19] M. Hiramatsu, K. Shiji, H. Amano, and M. Hori, "Fabrication of vertically aligned carbon nanowalls using capacitively coupled plasma-enhanced chemical vapor deposition assisted by hydrogen radical injection," *Applied Physics Letters*, vol. 84, no. 23, pp. 4708–4710, 2004.

[20] A. T. H. Chuang, J. Robertson, B. O. Boskovic, and K. K. K. Koziol, "Three-dimensional carbon nanowall structures," *Applied Physics Letters*, vol. 90, no. 12, Article ID 123107, 2007.

[21] H. Al-Mumen, F. Rao, W. Li, and L. Dong, "Singular sheet etching of graphene with oxygen plasma," *Nano-Micro Letters*, vol. 6, no. 2, pp. 116–124, 2014.

[22] A. L. M. Reddy, S. R. Gowda, M. M. Shaijumon, and P. M. Ajayan, "Hybrid nanostructures for energy storage applications," *Advanced Materials*, vol. 24, no. 37, pp. 5045–5064, 2012.

[23] X. Ling, L. Xie, Y. Fang et al., "Can graphene be used as a substrate for Raman enhancement?" *Nano Letters*, vol. 10, no. 2, pp. 553–561, 2010.

[24] Y. Wang, Z. Ni, H. Hu et al., "Gold on graphene as a substrate for surface enhanced Raman scattering study," *Applied Physics Letters*, vol. 97, no. 16, Article ID 163111, 2010.

[25] K. Jasuja and V. Berry, "Implantation and growth of dendritic gold nanostructures on graphene derivatives: electrical property tailoring and Raman enhancement," *ACS Nano*, vol. 3, no. 8, pp. 2358–2366, 2009.

[26] P. J. Wang, D. Zhang, L. S. Zhang, and Y. Fang, "The SERS study of graphene deposited by gold nanoparticles with 785 nm excitation," *Chemical Physics Letters*, vol. 556, pp. 146–150, 2013.

[27] L. Kou, H. He, and C. Gao, "Click chemistry approach to functionalize two-dimensional macromolecules of graphene oxide nanosheets," *Nano-Micro Letters*, vol. 2, no. 3, pp. 177–183, 2010.

[28] E. D. Palik, *Handbook of Optical Constants of Solids, Volumes I, II, and III: Subject Index and Contributor Index*, chapter 3, Elsevier Science & Technology, Riverport Ln Maryland Heights, Mo, USA, 1985.

[29] J. W. Weber, V. E. Calado, and M. C. M. van de Sanden, "Optical constants of graphene measured by spectroscopic ellipsometry," *Applied Physics Letters*, vol. 97, no. 9, Article ID 091904, 2010.

[30] J. A. Scholl, A. L. Koh, and J. A. Dionne, "Quantum plasmon resonances of individual metallic nanoparticles," *Nature*, vol. 483, no. 7390, pp. 421–427, 2012.

[31] M. S. Tame, K. R. McEnery, Ş. K. Özdemir, J. Lee, S. A. Maier, and M. S. Kim, "Quantum plasmonics," *Nature Physics*, vol. 9, no. 6, pp. 329–340, 2013.

[32] H. Yan, T. Low, W. Zhu et al., "Damping pathways of mid-infrared plasmons in graphene nanostructures," *Nature Photonics*, vol. 7, no. 5, pp. 394–399, 2013.